Cell, Vol. 82, 631–641, August 25, 1995, Copyright © 1995 by Cell Press

Cleavage Orientation and the Asymmetric Inheritance of Notch1 Immunoreactivity in Mammalian Neurogenesis

Anjen Chenn and Susan K. McConnell
Department of Biological Sciences
Stanford University
Stanford, California 94305

Summary

Neurons in the mammalian central nervous system are generated from progenitor cells near the lumen of the neural tube. Time-lapse microscopy of dividing cells in slices of developing cerebral cortex reveals that cleavage orientation predicts the fates of daughter cells. Vertical cleavages produce behaviorally and morphologically identical daughters that resemble precursor cells; these symmetric divisions may serve to expand or maintain the progenitor pool. In contrast, horizontally dividing cells produce basal daughters that behave like young migratory neurons and apical daughters that remain within the proliferative zone. Notch1 immunoreactivity is distributed asymmetrically in mitotic cells, with Notch1 inherited selectively by the basal (neuronal) daughter of horizontal divisions. These results provide cellular and molecular evidence that cortical neurons are generated from asymmetric divisions.

Introduction

The mammalian neural tube generates a large diversity of neuronal phenotypes during development. The developing nervous system must initially expand the number of precursor cells that populate its different regions, then generate neurons while replenishing the progenitor pool. Here we explore the mechanisms by which the production of neurons and progenitor cells is regulated during the development of the cerebral cortex. The cortex is composed of layers of neurons that are responsible for our highest cognitive and perceptual abilities. Cortical neurons are produced from progenitor cells in the ventricular zone, a pseudostratified columnar epithelium lining the lumen of the cerebral vesicles. The normal behavior of cortical progenitor cells has been described by using [^{3}H]thymidine to track the cell movements during the cell cycle (Sidman et al., 1959; Fujita, 1964). Replication of DNA during S phase is accomplished in the outer (basal) third of the ventricular zone (Figure 1A). In G2, nuclei translocate apically toward the lumenal surface, where they proceed through mitosis. Postmitotic neurons then migrate away from the ventricular zone. Prior to the onset of neurogenesis, it is thought that symmetric divisions in which both daughter cells reenter the cell cycle after mitosis serve to expand the pool of progenitor cells (Berry and Rogers, 1965; Smart, 1973; Gray and Sanes, 1992; Caviness et al., 1995). Neurogenesis begins slowly: neurons are born initially in small numbers that then build and peak late in neurogenesis (Miller, 1985; Caviness et al., 1995). Indirect evidence suggests that neurons can arise from asymmetric divisions, since clonally related neurons can span many layers (Luskin et al., 1988; Price and Thurlow, 1988; Walsh and Cepko, 1988), yet the layers are generated at distinct times in development (reviewed by McConnell, 1988a; Rakic, 1988). These observations have generated the proposal that an early precursor may produce both a neuron destined for an early-produced layer and another progenitor cell that then continues cycling to produce neurons destined for later-generated locations.

This hypothesis raises the question of whether the behavior of dividing cells predicts whether neurons, progenitor cells, or both are generated from a given division. Several authors have speculated that the orientation of mitotic cleavage may regulate the production of neurons (Langman et al., 1966; Martin, 1967). Horizontal cleavage planes would bisect a progenitor cell into an apical and basal daughter, the latter of which is untethered to the lumenal surface and conceivably free to migrate away and differentiate into a neuron (Figure 1C). The daughters of vertical cleavages, in contrast, would both be attached to the ventricular surface and would perhaps be more likely to continue to proliferate (Figure 1B). Despite the appeal of these hypotheses, previous studies of cleavage orientation in fixed sections through the cerebral ventricular zone have suggested that the vast majority (~90%) of all cleavages are oriented vertically even during peak periods of neuronal production (Smart, 1973; Zamenhof, 1986), leading many to doubt the significance of cleavage orientation in neurogenesis (Hinds and Ruffett, 1971; Smart, 1973).

To examine the regulation of the numbers of neurons and progenitor cells during development, we have visualized the behavior of dividing precursors during and preceding the major period of neurogenesis in the developing cerebral cortex of the ferret, Mustela furo, a mammal in which neurogenesis occurs both pre- and postnatally (McConnell, 1988b). By imaging of living cells, we find evidence for asymmetric divisions that result in the production of a neuron and another progenitor cell. In addition, we provide evidence that *Notch1*, a mammalian homolog of the Drosophila melanogaster *Notch* gene, is asymmetrically localized within dividing progenitor cells and inherited differentially following asymmetric divisions.

Results

Determination of Cleavage Angles in Fixed Sections

To examine the angles at which progenitor cells undergo cleavage in the developing cerebrum, sections from embryonic day 29 (E29) ferret brains (early in neurogenesis) were stained with a monoclonal antibody to α-tubulin that reveals microtubules, including those of the mitotic spindle. Metaphase spindles were seen at a variety of orientations: although most suggested cleavage planes roughly vertical or perpendicular to the ventricular surface (Figure

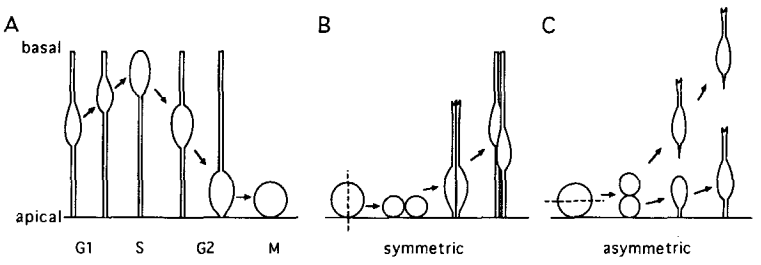

Figure 1. Interkinetic Nuclear Migration and Models for Symmetric and Asymmetric Division of Neuronal Precursors

(A) Ventricular cell nuclei undergo intracellular migration during the cell cycle. In G1, the nucleus ascends away from the apical surface. S phase nuclei are located in the outer (basal) third of the ventricular zone. During G2, nuclei translocate apically, and mitosis occurs at the ventricular surface.

(B) A vertical cleavage (perpendicular to ventricular surface) gives rise to two daughters that sit side by side, both retaining apical connections. Both daughters rise away together from the lumen slowly and may reenter the cell cycle.

(C) A horizontal (parallel) cleavage produces an apical daughter (bottom arrow) that retains contact with the apical surface and a basal daughter (top arrow) that loses contact with the lumen. The apical daughter may be constrained to stay in the epithelium, while the basal daughter migrates away.

2A), some were horizontal or parallel to the lumenal surface (Figure 2B, arrowhead), and others were oblique (Figure 2B, arrow). The orientations of projected cleavage planes were tabulated for 102 mitotic cells. In contrast with previous reports for mouse suggesting that at least 90% of cleavages are vertical (Smart, 1973), only 70% of cells in the present study were oriented vertically (60°–90°; Figure 2C). The remaining cleavage planes were distributed evenly among all other possible orientations, with roughly 15% horizontal (0°–30°).

These data suggest that horizontal cleavages are more common in the cortical ventricular zone than thought previously and raise the possibility that such cleavages might be intimately connected with neurogenesis. We worried, however, that these figures might misrepresent actual cleavage angles if metaphase plates rotated within cells prior to division. In addition, static methods cannot reveal the behavior of daughter cells generated from vertical cleavages versus that of cells generated from horizontal cleavages. We therefore developed a slice system to follow the behavior of dividing cells and their daughters in tissues that maintain salient features of their normal three-dimensional environment (O'Rourke et al., 1992; Dailey et al., 1994). Bromodeoxyuridine labeling revealed that interkinetic nuclear migration occurs normally in cortical slices (data not shown).

Time-Lapse Imaging of DiI-Labeled Progenitor Cells

To visualize dividing cortical precursor cells and their daughters, we injected dilute solutions of the fluorescent lipophilic tracer 1,1′-dioctadecyl-3,3,3′,3′-tetramethylindocarbocyanine perchlorate (DiI) into the lateral ventricles of E29 ferrets, labeling single progenitors or small clusters of ventricular cells. Slices derived from these brains were imaged with time-lapse confocal microscopy. During the imaging period, 40 DiI-labeled cells (21 slices from 21 animals) divided and were followed for up to 25 hr after division. We measured the cleavage angle of each cell that divided and assigned the cell into one of three groups: vertical cleavage planes (60°–90°), horizontal cleavage planes (0°–30°), and intermediate orientations (30°–60°). Because DiI labels the cell plasma membrane, it was sometimes difficult to assess precisely the angle of cleavage; cells included here fit clearly into one category as assessed by three independent observers. The majority (35 of 40) of dividing cells displayed behaviors both during and following cleavage that could be classified into two distinct patterns, described below.

Symmetric Divisions

The predominant mode of division in E29 ferret slices was one in which progenitor cells divided with vertical cleavage planes. Figures 3A–3H show an example of one such cell

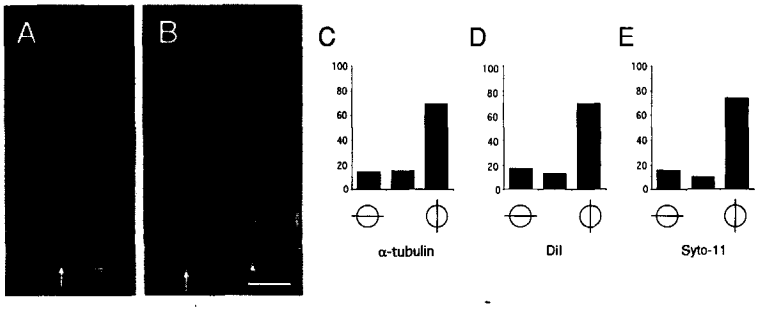

Figure 2. Visualization of Microtubules Reveals Mitotic Spindle Orientation of Dividing Precursors

(A and B) Confocal images of E29 ferret cerebral ventricular zone stained with an antibody against α-tubulin. The ventricular (apical) surface is down.

(A) The orientation of a mitotic spindle (arrow) suggests that this cell will divide with a vertical cleavage plane.

(B) The cell on the right (arrowhead) may divide horizontally. The left-hand cell (arrow) appears to be dividing at an oblique angle of about 45°. Scale bar, 10 μm.

(C–E) Histograms comparing the relative frequencies of vertical (60°–90°), intermediate (30°–60°), and horizontal (0°–30°) cleavages at E29 in fixed sections stained for mitotic spindles, and time-lapse sequences of dividing progenitors labeled with DiI or Syto-11.

(C) In fixed sections, 69.5% of mitotic spindles formed vertical cleavage planes; 14.5% were horizontal (n = 103 cells).

(D) A similar distribution of cleavage angles was obtained from living progenitors labeled with DiI (see Figure 3): 70% divided with vertical cleavage planes, and 17.5% divided horizontally (n = 40 cells).

(E) Time-lapse imaging of dividing cells labeled with Syto-11 (see Figure 4): 74% were vertically oriented and 16% were horizontal (n = 113 cells).

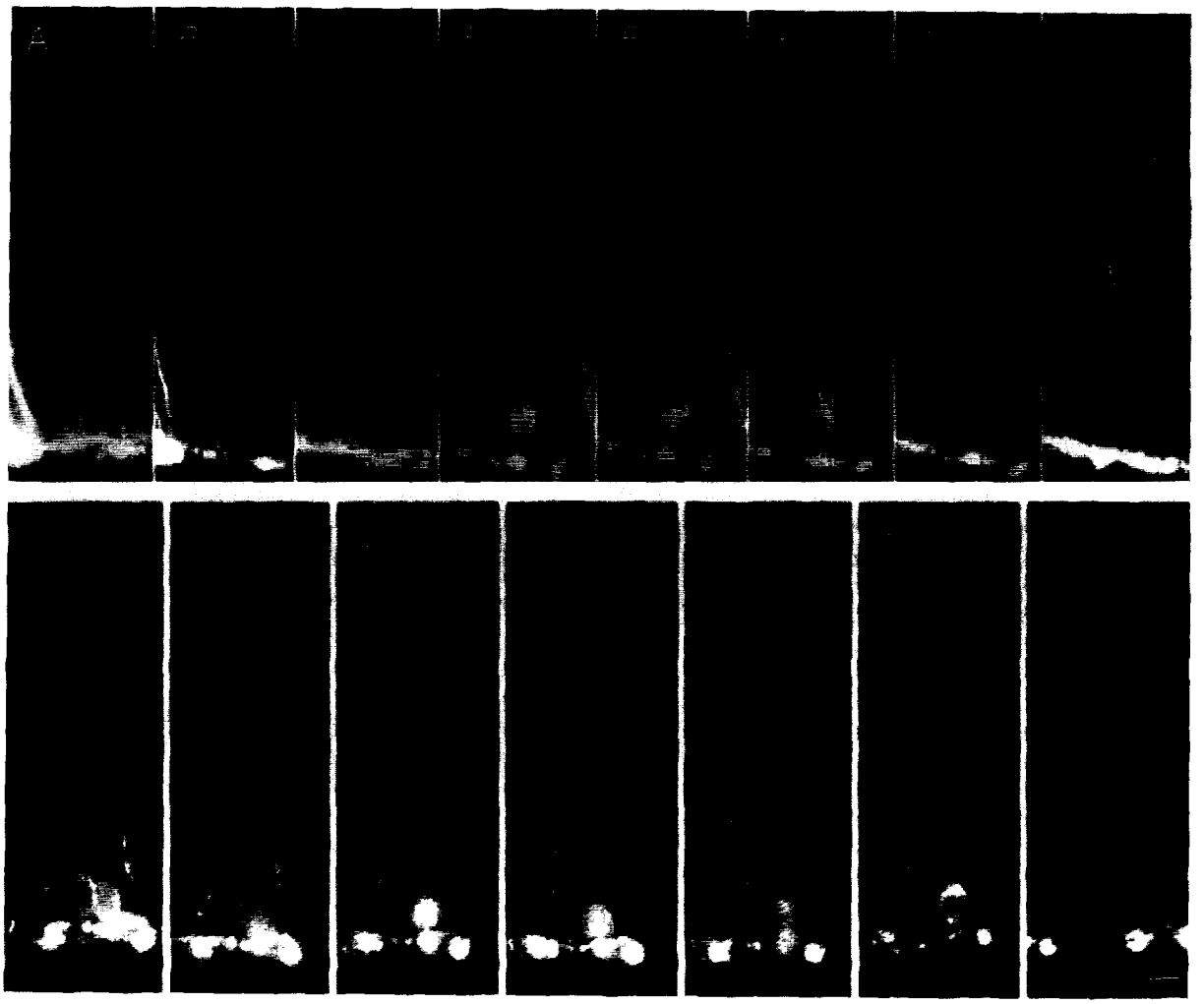

Figure 3. Time-Lapse Imaging of DiI-Labeled Progenitor Cells

DiI-labeled progenitor cells in the E29 ventricular zone visualized with time-lapse confocal microscopy. Each frame represents a single optical section from a time-lapse series of images. The ventricular (apical) surface is down.

(A–H) Interkinetic nuclear migration and vertical cell division. The cell marked with an arrow in (A) exhibits the typical bipolar morphology of a progenitor cell, with an elongated nucleus and radially oriented processes extending toward the ventricular and pial surfaces.

(B–D) The nucleus descends rapidly to the ventricular surface during G1 (28 μm/hr). Cytokinesis occurs between (D) and (E), with a vertical cleavage orientation (90°).

(F–H) Following mitosis, both daughters maintain a close contact with one other, and their cell bodies rise away slowly (5.4 μm/hr) from the lumen. Both readopt the characteristic bipolar morphology of a progenitor cell, each appearing to maintain a thin cytoplasmic process contacting the lumenal surface. Times in each panel: (A), 0 hr; (B), 2.1 hr; (C), 3.3 hr; (D), 3.8 hr; (E), 4.3 hr; (F), 5.3 hr; (G), 10.7 hr; (H), 15.4 hr. Scale bar, 10 μm.

(I–O) A horizontal division followed by migration of the basal daughter away from the ventricular zone.

(I–J) A labeled cell (arrow) at the lumenal surface divides with a horizontal cleavage plane (0°). The basal daughter (top arrow) apparently lacks contact with the ventricular (apical) surface.

(K) Following cleavage, both cells rise away from the lumen.

(L) Later, 4.6 hr following cleavage, the basal (top) daughter separates from its sister.

(M–O) Still later, at 15.5 hr after division, the top daughter migrates away at a rapid rate of 37 μm/hr. The position of the apical daughter (out of plane of focus but visualized separately) is marked with the bottom arrow. Times in each panel: (I), 0 hr; (J), 0.8 hr; (K), 4.2 hr; (L), 5.4 hr; (M), 12.2 hr; (N), 17.8 hr; (O), 18.3 hr. Scale bar, 10 μm.

imaged over a total period of 15.4 hr. Initially, this cell showed the typical bipolar appearance of a cortical progenitor, with thin processes extending both basally and apically toward the pial and lumenal surfaces, respectively (Figure 3A). Over time, the cell nucleus slid apically within the cytoplasm toward the ventricular surface (Figures 3A–3C). As the nucleus reached the lumen (Figure 3D), the cell appeared to withdraw its pial process and round up in preparation for cytokinesis. The cleavage that followed was vertically oriented, generating two daughters sitting side by side (Figure 3E). Over the following 11 hr, the sibling cells maintained a close proximity to one another, their somata in apparent contact as their nuclei migrated slowly outward (Figures 3F–3H). The cells reestablished

Table 1. Cleavage Orientation at E29 and the Behavior of Daughter Cells Following Mitosis

Cleavage Angle (Degrees)	Cell Divisions Imaged (Percent)	Divisions in Which Daughters Separated after Cleavage (Percent)	Average Rate of Outward (Basal) Movement after Cleavage (μm/hr)			Average Time Interval between Cleavage and Separation (hr)	Average Time Cells Were Imaged after Cleavage (hr)
			Of Daughters That Separated		Of Daughters That Remained Together		
			Basal	Apical			
0–30	7 of 40 (17.5)	6 of 7 (85.7)	10.2	1.0	1.0	2.6	11.3
30–60	5 of 40 (12.5)	1 of 5 (20.0)	21.0[a]	5.6[a]	3.9	0.9[a]	5.7
60–90	28 of 40 (70.0)	3 of 28 (10.7)	6.2	3.0	5.6	7.4	7.0

[a] Data are from the single cell division in which separation was observed.

a bipolar morphology during this period and appeared to retain contact with the ventricular surface.

At E29, 28 of 40 cells imaged had cleavage orientations of 60°–90° (Table 1). We classify these divisions as symmetric, on the basis of their morphology and behavior following division. By DiI labeling, each daughter appears to maintain contact with the ventricular surface (Figure 3E), and inspection of fixed semi-thin sections reveals telophase cells in which both daughters have ventricular contacts (see Figure 6). In addition, published electron micrographs suggest that vertical divisions result in the segregation of apical components roughly equally to both daughters (Hinds and Ruffett, 1971). Strikingly, in almost 90% of these cases, the two daughters generated from such divisions maintained close contact with one another as their nuclei moved outward within the ventricular zone. The average rate of movement of this paired outward migration was 5.6 μm/hr (Table 1). Only 3 of 28 vertical divisions generated daughters that separated after mitosis. In these cases, the rates of outward movement of each daughter were similar (Table 1). Overall, the rates of outward or basal movement after mitosis were slow compared with the average rate of inward or apical movement. G2 cells descending to the ventricular surface prior to mitosis moved at an average rate of 18.3 μm/hr and sometimes moved at rates exceeding 40 μm/hr. These data are consistent with previous suggestions that the rates of apical nuclear movements in G2 exceed the basal rates of G1 nuclear migration (Takahashi et al., 1993).

Asymmetric Divisions

A second mode of cell division in E29 slices was observed in about 18% of divisions, in which progenitor cells divided with horizontal cleavage planes (Table 1). One such cell was rounded up at the ventricular surface in preparation for mitosis at the start of the imaging period (Figure 3I). Cleavage occurred at an angle of ~0° (Figure 3J), generating an apically and a basally placed daughter. Although both daughters initially elongated in the radial direction (Figure 3K), the basal (outer) sibling rapidly extended a pial process but had no apparent connection with the ventricular surface. At 4.6 hr after cleavage, the two daughters separated (Figure 3L), and the basal cell spent several hours within 1–3 cell diameters of its sibling, which moved outward very slowly during this period. At 15.5 hr after division, however, the basal daughter suddenly began to migrate quite rapidly (37 μm/hr) outward toward the pial surface, leaving its sibling behind (Figures 3M–3O). Although the morphological features of this cell are not clear at single time points, time-lapse viewing revealed a thick and dynamic leading process and elongated nucleus, similar to migrating neurons in the intermediate zone of cortical slices (O'Rourke et al., 1992).

Using the same logic mapped out for vertical divisions, we classify horizontal divisions as asymmetric. First, daughters generated from such divisions exhibit striking morphological differences from one another. The apical daughter appears to retain contact with the ventricular surface, while the basal cell has no obvious lumenal contact after cleavage (Figure 3J; data not shown). Electron microscopy of a horizontally dividing cortical cell in telophase indicates that an apical cell can inherit the entire apical surface from its progenitor (Hinds and Ruffett, 1971). Second, daughters generated from horizontal divisions behave in strikingly different ways from one another: six out of seven horizontal divisions produced sibling pairs that separated after cleavage. While apical daughters moved outward very slowly (1.0 μm/hr on average), the average rate of movement of basal cells was about 10 times faster (10.2 μm/hr), exceeding that of vertically derived daughters (Table 1) and approximating the rate at which young neurons migrate to the cortex (Hicks and D'Amato, 1968; McConnell, 1988b; O'Rourke et al., 1992). This average rate masks the maximal velocities of movement in cells that bolted from their siblings (e.g., Figures 3M–3O): in two cases, basal daughters moved at very high speeds (37 and 33 μm/hr), a behavior that was never observed for cells derived from vertical divisions. In general, daughters generated from horizontal cleavages separated from one another soon after division (average, 2.6 hr; Table 1). In contrast, in the few cases in which the daughters derived from vertical cleavages separated, the cells did so only after a long period of time (average, 7.4 hr).

Intermediate Orientations

The remaining cells (5 of 40) divided at intermediate angles (30°–60°). Of these, one generated daughters that separated 0.9 hr after cleavage, as in a horizontal division. The basal daughter migrated rapidly toward the pial surface

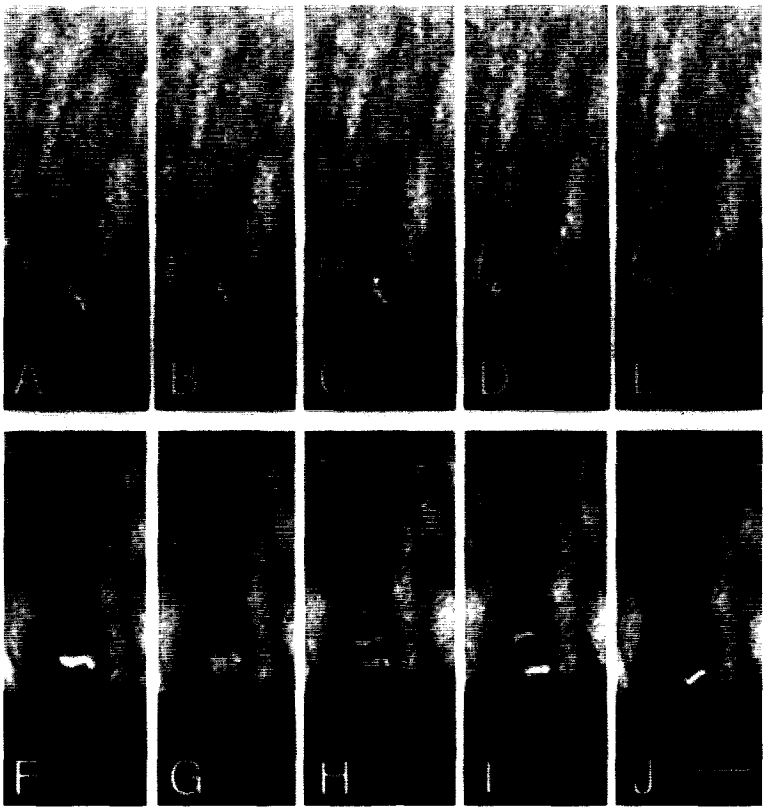

Figure 4. Time-Lapse Imaging of Syto-11-Labeled Progenitor Cells

Time-lapse confocal imaging of cortical slices labeled with Syto-11. Labeling was diffuse until chromatin condensation in metaphase, at which time a bright bar of fluorescence indicated the position and orientation of the metaphase plate.

(A–E) A vertical division in an E29 slice. In this cell, the metaphase plate rotates nearly 45° clockwise (A–C) prior to chromatid separation (D). The chromatids separate vertically (90°) at anaphase (D and E). Times in each panel: (A), 0 min; (B), 2 min; (C), 4 min; (D), 10 min; (E), 12 min.

(F–J) A horizontal division in an E36 slice. A brightly labeled metaphase plate is visible in (F). The sister chromatids then separate with a plane of division of approximately 0° (G, H). Following division, the basal daughter has apparently migrated out of the focal plane, although the apical daughter is still visible (J, arrowhead). Times in each panel: (F), 0 min; (G), 7 min; (H), 9 min; (I), 13 min; (J), 25 min. Scale bar, 10 μm.

(21.0 μm/hr), while the apical daughter moved relatively slowly (5.6 μm/hr). This division thus appeared to fall into the asymmetric category. The remaining four divisions produced daughters that stayed together and moved slowly from the lumenal surface, as in a symmetric division. We do not know what cleavage angle is necessary to create asymmetric daughters, but electron micrographs of oblique divisions (Hinds and Ruffett, 1971) suggest that angles up to 45° can result in one daughter losing contact with the lumenal surface.

Determination of Cleavage Orientations over Time

These data generate the proposal that early in cortical development, horizontal divisions produce young neurons, and vertical divisions replenish the progenitor pool. Were this hypothesis correct, one would expect a strong correlation between the fraction of horizontal divisions and the extent of neuronal production at different times during development. No horizontal cleavages should occur prior to the onset of neurogenesis. As neurogenesis proceeds, the fraction of cells that differentiate into neurons after mitosis increases steadily (Caviness et al., 1995); thus, increasing numbers of horizontal divisions should be observed. To visualize the entire population of ventricular cells and determine cleavage orientations with precision at a variety of ages, we labeled the chromosomes of cells in living slices with Syto-11, a vital nucleic acid–binding dye. Syto-11 revealed metaphase plates and the orientations of chromosome separation clearly (Figure 4). The advantages of this method include universal labeling and accurate assessment of cleavage angles at a variety of ages; a disadvantage was that the behavior of daughter cells could not be tracked after division and chromosome decondensation, since progeny then blended into the labeled population.

Syto-11 staining revealed both vertical and horizontal cleavages (Figure 4). In one cell that divided vertically, the metaphase plate rotated within the cell soma prior to cleavage (Figures 4A–4C), a behavior that was observed occasionally in other cells. Following cleavage, both daughter cells appear to undergo chromosome decondensation at roughly the same time, their diffusely labeled nuclei becoming indistinguishable from surrounding cells (data not shown). In a horizontal cleavage (0°; Figures 4F–4J), the two daughters appeared to separate rapidly from one another following cleavage, since the apical daughter is visible at the ventricular surface, whereas the basal daughter has disappeared (Figure 4J). This behavior is not unexpected given the results of imaging DiI-labeled cells.

We imaged the divisions of Syto-11-labeled cells at three times during cortical neurogenesis: E29 (early neurogenesis; layer 6 neurons are being born), E36 (midneurogenesis; layer 4), and P1–3 (late neurogenesis; layer 2/3). At each age, the angle of cleavage was determined for a population of about 50 or more cells and classified as horizontal, intermediate, or vertical (see Figure 6). At E29, most divisions (74%) were vertically oriented, about 16% were horizontal, and 10% were intermediate. Similar percentages were observed at E36, with roughly 73% vertical

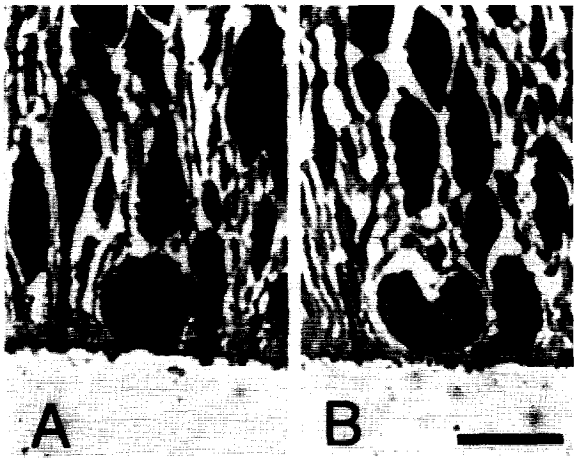

Figure 5. Mitotic Cleavage Orientations of Progenitors during the Period Prior to Neurogenesis

Semi-thin plastic sections of E20 cerebral wall stained with toluidine blue to reveal the orientations of mitotic cells in anaphase or telophase.
(A) A vertically dividing cell in mid-anaphase.
(B) A cell in early telophase with a vertical cleavage furrow between the two future daughter cells, each of which retains an apical contact.
Scale bar, 10 μm.

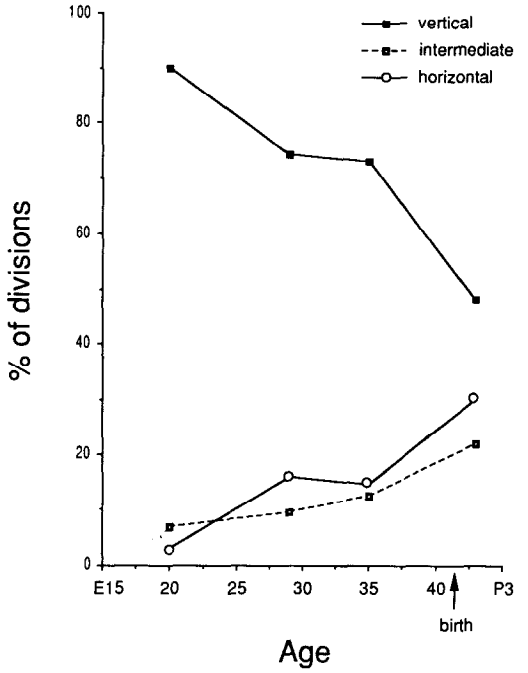

Figure 6. Distributions of Mitotic Cleavage Orientations before and during Neurogenesis

Cleavage angles of Syto-11-labeled progenitor cells at E29 (113 divisions, 6 slices), E36 (48 divisions, 11 slices), and P1–3 (50 divisions, 17 slices). Because we could not image dynamic movements in E20 brains, the orientations of mitotic cells in fixed semi-thin sections were measured (100 cells, 3 brains; see Figure 5). Divisions were categorized as horizontal (0°–30°; circles), intermediate (30°–60°; open squares), and vertical (60°–90°; closed squares).

divisions. In contrast, at neonatal ages, fewer than half of all divisions (48%) were vertical, and the frequency of horizontal divisions roughly doubled, to 30%. These data are consistent with the prediction that horizontal divisions should occur during the period of neurogenesis and that their frequency should increase over time.

We attempted to image Syto-11-labeled cells in E20 slices, prior to the onset of neurogenesis, but were unsuccessful, owing to the small size of the telencephalon at this age. To acquire data on cleavage orientation from the early cortex, we prepared semi-thin (0.5 μm) plastic-embedded sections from E20 embryos and measured the cleavage orientations of toluidine blue–stained cells in late anaphase or telophase of the cell cycle. Metaphase figures were excluded, since metaphase plates can rotate prior to division (Figure 4). Two vertically dividing cells are shown in Figure 5: one cell is in anaphase (Figure 5A), and the other, in which a cleavage furrow is evident, is beginning telophase (Figure 5B). As predicted, nearly all dividing cells (90%) were found with cleavage planes of roughly 90° (Figure 6). Only 3% of cells divided horizontally, and 7% had intermediate orientations. Thus, the occurrence of horizontal divisions strongly correlates with the generation of neurons.

Collectively, these data support the hypotheses that vertical divisions are symmetric and proliferative in nature, and that horizontal divisions are asymmetric and differentiative, resulting in the production of a postmitotic neuron. While it might be worrisome that cleavage orientations are compared by using two different methods in Figure 6, we feel confident that each method reflects accurately the pattern of cleavages seen in vivo. At E29, the distributions of cleavage orientations of living cells imaged both with DiI and Syto-11 are essentially identical to those of cells viewed in fixed sections stained with antibodies to reveal mitotic spindles (see Figures 2C–2E). Thus, the mitotic behavior of cells in slices is indistinguishable from that of their counterparts fixed in vivo.

Asymmetric Localization of Notch1 Protein in Dividing Progenitor Cells

To explore the possibility that asymmetric divisions result from the differential inheritance of cytoplasmic or membrane-bound determinants (Rhyu et al., 1994), we examined the distribution of several proteins hypothesized to play a role in neural cell fate decisions. The gene encoding one such protein, *Notch1*, is expressed at high levels in the cerebral ventricular zone (Weinmaster et al., 1991, 1992). In Drosophila, the *Notch* gene encodes a large transmembrane protein involved in a variety of cell fate choices, including the decision to become a neuron versus an epidermal cell (Artavanis-Tsakonas et al., 1995). *Notch1* has also been implicated in the control of neurogenesis in vertebrates (Coffman et al., 1993; Swiatek et al., 1994; Dorsky et al., 1995).

We stained sections through the ferret ventricular zone with monoclonal antibodies specific to distinct epitopes of the intracellular domain of human Notch1 (antibodies TAN1-20G and TAN1-18G from P. Zagouras and S. Artavanis-Tsakonas; similar staining patterns were obtained with each antibody, suggesting that the antigen revealed is Notch1 or a closely related protein). Strong Notch1 im-

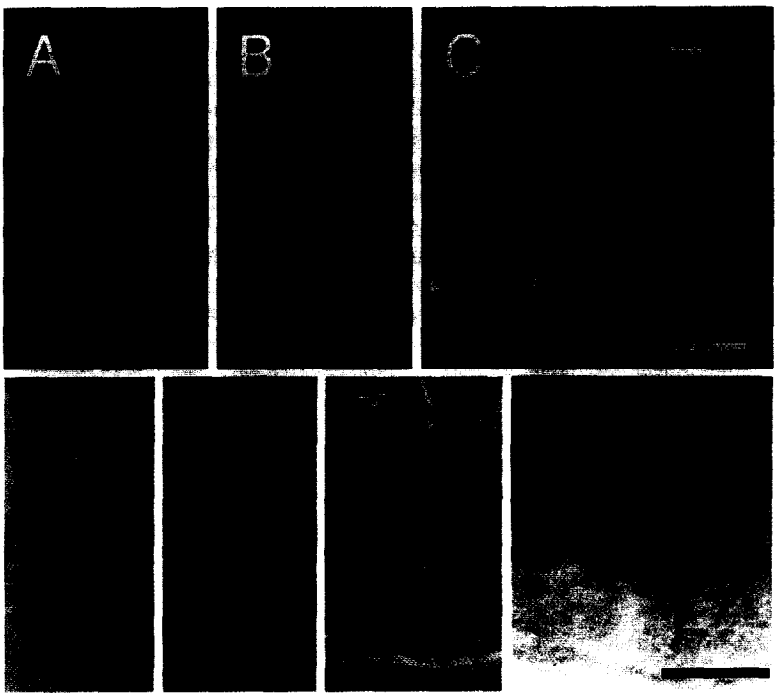

Figure 7. Notch1 Is Asymmetrically Localized in Mitotic Cells and Asymmetrically Inherited during Horizontal Cleavage

Notch1 immunoreactivity, revealed with the TAN1-20G antibody, is seen in the basal portion of mitotic cells in metaphase and anaphase, regardless of cleavage orientation.

(A–C) Confocal images of E29 ventricular cells, showing Notch1 immunoreactivity (revealed with Cy-5, pseudocolored red) and nuclear morphology (propidium iodide, pseudocolored green).

(A) Notch1 staining (red) is concentrated at the basal pole of a metaphase cell. The metaphase plate, stained by propidium iodide (green), is oriented vertically. Of 55 metaphase cells at E29, basal Notch1 staining was apparent in 73%.

(B) A basal crescent of Notch1 immunoreactivity in a rounded mitotic cell.

(C) Notch1 staining is found in a basal cap in an anaphase cell undergoing horizontal division (arrowheads mark predicted cleavage plane). Of 6 anaphase cells, 5 showed basal Notch1 staining, including all undergoing horizontal cleavage. Another cell expressing Notch1 basally is seen at a distance from the lumenal surface (arrow).

(D–G) Sections immunostained for Notch1, visualized by using a diaminobenzidine reaction, and counterstained with toluidine blue (D and E).

(D) An E29 cell in late anaphase shows basal Notch1 staining (brown), suggesting an equal distribution of Notch1 to the two daughters.

(E) Asymmetric Notch1 localization in an early anaphase cell at E29 with a cleavage orientation of 45°. Arrowheads mark the predicted cleavage orientation; Notch1 may be distributed asymmetrically to the basal daughter of this division.

(F) A horizontally dividing E36 cell in early telophase. Arrowheads mark the cleavage furrow. Notch1 staining is associated exclusively with the basal daughter, suggesting that Notch1 is inherited asymmetrically in horizontal divisions. Only a third of telophase cells showed clear Notch1 staining, possibly due to the rapid reextension of a pial process in vertically dividing cells. (G) A rounded cell (arrowhead) at E36 shows intense Notch1 immunoreactivity at a distance from the ventricular surface. These cells were viewed only rarely, but were conceivably derived from horizontal divisions. Slightly out of the plane of focus is a mitotic cell with basal Notch1 staining (arrow). Paraffin sections were used in (A)–(E), and cryosections for (F)–(G).

Scale bar in (C), 10 μm, for (A)–(C); scale bar in (G), 10 μm, for (D)–(G).

munoreactivity is localized to cells rounded up at the ventricular surface for mitosis. Staining was strikingly asymmetric in distribution: Notch1 immunoreactivity is localized to the basal portion of mitotic cells, with little or no staining apically (Figure 7). This distribution is seen in progenitor cells regardless of their projected angle of cleavage: Notch1 is concentrated in the basal half of cells initiating or progressing through mitosis at angles ranging from vertical (Figures 7A and 7D) to horizontal (Figures 7C and 7E). Of 61 cells in metaphase or anaphase of the cell cycle, 74% showed a basal cap of Notch1 staining; no staining was visible in the remaining cells. This distribution suggests that cells dividing with horizontal cleavage planes should generate molecularly distinct daughters: an apical daughter that lacks Notch1 and a basal daughter that inherits the bulk of this protein. In support of this view, Figure 7F shows a progenitor cell in telophase of a horizontal cleavage, with Notch1 immunoreactivity associated exclusively with the basal daughter.

Although Notch1 staining is highly concentrated in metaphase and anaphase cells, it is less apparent at other stages of the cell cycle. Of 34 cells in prophase or prometaphase, only 26% displayed a basal cap of Notch1 staining. Interphase cells exhibit low levels of immunoreactivity visible on their thin bipolar processes within the ventricular zone (data not shown). Little or no staining is visible at apical surfaces. These observations suggest that at most stages of the cell cycle, Notch1 is distributed diffusely over the basolateral cell surface. As the pial process of the progenitor cell collapses during prometaphase (Hinds and Ruffett, 1971), formerly diffuse Notch1 protein may become highly concentrated in a crescent at the basal pole of the cell. It is also conceivable that the intense Notch1 staining of mitotic cells represents the synthesis of new Notch1 protein just before mitosis; *Notch1* mRNA is distributed, however, throughout the entire ventricular zone (Weinmaster et al., 1991), apparently in cells at all stages of the cell cycle. We do not know whether the formation of the basal crescent of Notch1 simply concentrates this protein in an exaggerated form of its normal basolateral pattern, whether some Notch1 protein is actively moved to the basal pole as the cell rounds up in preparation for mitosis, or whether the protein is capped owing to ligand binding. Finally, although the vast majority of cells that showed heavy Notch1 staining were mitotic cells located at the lumenal surface, we occasionally viewed cells expressing intense Notch1 immunoreactivity at a distance from the lumen (Figures 7C and 7G). It is possible that these cells were the basal daughters of horizontal cleavages.

Mammalian ventricular cells are markedly polarized, with a single cilium, an associated centrosome, and zonula adherens junctions at the apical surface (Stensaas and Stensaas, 1968; Hinds and Ruffett, 1971). Several proteins that play important roles in signaling among epithelial cells in Drosophila are localized apically, including Notch, sevenless, boss, and armadillo, among others (reviewed by Woods and Bryant, 1993). We decided to explore the localization of Notch, a protein implicated in the control of neurogenesis in both flies and vertebrates (Artavanis-Tsakonas et al., 1995), in mammalian ventricular cells. To our surprise, Notch1 immunoreactivity is indeed localized asymmetrically in dividing progenitors, but is found basally (or basolaterally) rather than apically. Because Notch1 is concentrated in a basal cap regardless of cleavage orientation, only those cells dividing horizontally will differentially distribute Notch1 to the two daughters (Figure 7F). The asymmetric inheritance of Notch1 may provide or contribute to the molecular mechanisms for the production of two distinct cell types from a single division.

In contrast with *numb* and *prospero*, which regulate cell fates intrinsically, *Notch* plays a role in the regulation of local cell signaling (Artavanis-Tsakonas et al., 1995). In Drosophila, *Notch* mutants form too many neuroblasts, apparently owing to the failure of emerging neuroblasts to inhibit their neighbors from adopting a neural fate (Doe and Goodman, 1985; Artavanis-Tsakonas et al., 1995). Expression of an activated form of Notch blocks neurogenesis in the ventral neurogenic region without affecting epidermal development (Struhl et al., 1993). It is thus surprising that we find Notch1 staining segregated to the basal (neuronal) daughter of a horizontal cleavage, since Notch activity is associated with the suppression of neuronal differentiation in vertebrate systems as well (Coffman et al., 1993; Nye et al., 1994; Dorsky et al., 1995). Such results have generated the hypothesis that Notch signaling directs cells into a nonneuronal fate, an idea at apparent odds with our results.

It has been argued, however, that Notch plays a more general role in modulating the ability of a cell to respond to a variety of inductive signals (Artavanis-Tsakonas et al., 1995). Introduction of activated Notch in the compound eye of Drosophila, for example, blocks the normal induction of photoreceptor cells, causing cells either to adopt incorrect cell fates or to differentiate incompletely (Fortini et al., 1993). Artavanis-Tsakonas and colleagues (1995) have hypothesized that Notch activation freezes a cell in its current developmental state, deafening it to the reception of other developmental signals; thus, Notch activation may play a restrictive rather than instructive role in cell fate decisions. In addition, Notch immunoreactivity is found in a subset of terminally differentiated cells in the vertebrate retina, suggesting that in some cases Notch activity may serve to maintain the differentiated state (Artavanis-Tsakonas et al., 1995).

In the mammalian neural epithelium, the asymmetric inheritance of Notch1 may regulate differentially the responsiveness of two daughter cells to extrinsic cues. It is also conceivable that Notch1 activity prevents differentiation both in young neurons and in progenitor cells: newly generated neurons may require large amounts of Notch1 to delay differentiation long enough to escape the ventricular zone. It is interesting in this context that vertically dividing cells distribute Notch1 roughly equally to both daughters, suggesting that each retains Notch1 protein as it reenters the cell cycle. In horizontal divisions, the basal daughter appears to inherit the Notch1, leaving little if any for its apical sibling. Apical daughters of horizontal divisions move outward at extremely slow rates after division (Table 1), conceivably delaying their outward movement to express more Notch1 protein before reentering the cell cycle. Finally, it is possible that Notch1 plays an instructive role in ventricular cells, and that the differential inheritance of Notch1 biases cells toward distinct developmental outcomes. Transplantation studies suggest that cortical neurons make decisions about their laminar fate during or shortly after the S phase of their final cell cycle (McConnell and Kaznowski, 1991). If Notch1 activation simply restricts the competence of cells to respond to other cues, activating Notch in ventricular cells could generate distinct phenotypic outcomes depending on the position of the cell in the cell cycle at the time of activation. This hypothesis could be tested by the introduction of activated forms of Notch1 into ventricular cells at different stages of the cell cycle.

Regulation of the Prevalence of Asymmetric versus Symmetric Divisions over Time

The change in fraction of asymmetric cleavages observed before and during the period of neurogenesis suggests that nature has devised a mechanism by which to regulate cleavage orientations over time, but how cleavage angles might be regulated in a mammalian system presents a mystery. The regulation of cleavage orientation may have profound consequences for normal cortical development. If cleavage angles are not properly regulated, too many or too few neurons may be produced at a given time or in a given region. Cell death might compensate for the overproduction of neurons, but underproduction could lead to disaster. Since cell fate decisions are made prior to mitosis (McConnell and Kaznowski, 1991), it is conceivable that cleavage orientation is somehow controlled by this earlier decision.

Experimental Procedures

Immunohistochemistry

Microtubules were visualized by fixing E29 ferret brains by immersion in −20°C 90% methanol or perfusion with microtubule-stabilizing buffer (Schulze and Kirschner, 1986) at room temperature followed by 0.5% glutaraldehyde. Paraffin sections of 10 μm were blocked with 1% bovine serum albumin (BSA) in phosphate-buffered saline (PBS) (1 hr at room temperature) and incubated with mouse monoclonal antibody DM1α (Sigma; 1:500, 1 hr at room temperature), then with Texas red–conjugated donkey anti-mouse secondary (Jackson Laboratories; 1:200, 1 hr at room temperature). For Notch1 staining, E29 and E36 ferrets were perfused with 4% paraformaldehyde; 5 μm paraffin sections or 15 μm cryosections were blocked with 5% goat serum, 0.5% BSA, 0.1% Triton X-100 in PBS (30 min at room temperature), then incubated with TAN1-20G or TAN1-18G monoclonal antibodies (gifts of P. Zagouras and S. Artavanis-Tsakonas; 1:5 in blocking solution without BSA or undiluted; 2 hr at room temperature). Each antibody was generated to the intracellular domain of human Notch1, and

both cross-react with rat and mouse Notch1 (Artavanis-Tsakonas et al., 1995). Sections were incubated with biotinylated goat anti-rat secondary (Vector; 1:200 in PBS with 1 mg/ml BSA, 1 hr at room temperature), then ABC reagent (Vector), and counterstained with toluidine blue (1% in 1% borate buffer). For fluorescence, sections were incubated with biotinylated goat anti-rat secondary (Jackson; 1:200 in PBS, 1 mg/ml BSA, 1 hr at room temperature), then streptavidin-coupled Cy-5 (Jackson; 1:100 in PBS, 1 mg/ml BSA, 1 hr at room temperature) and counterstained with propidium iodide (Sigma; 5 μg/ml in PBS, 15 min at room temperature). Confocal images were merged with Adobe Photoshop. For quantitation of Notch1-immunoreactive cells, TAN1-20G-labeled cells were located in the E29 ventricular zone; all mitotic cells (n = 117) in those regions were identified with propidium iodide. Controls with no primary antibody showed no staining.

Time-Lapse Imaging

E29 progenitor cells were labeled by injection of 3 μl of DiI (0.5% DiI [DiIC18(3), Molecular Probes] in dimethylformamide, diluted 1:100 in high glucose Hanks' balanced salt solution [HBSS]) into the lateral ventricles by using a 30 gauge needle and Hamilton syringe. Coronal slices (400 μm) were prepared and placed on coverslips as described (Roberts et al., 1993), with the following changes: 1.5 ml of Gähwiler's medium or 1 × minimal essential medium (GIBCO) with 1 mM α-ketoglutarate, 100 U/ml penicillin (GIBCO), 100 mg/ml streptomycin (GIBCO) was used as media; slices placed onto coverslips were immediately covered with 25 μl of Vitrogen gel. After at least 2 hr in an incubator (5% CO_2, 37°C), slices were placed in a plastic chamber, covered with medium (33°–35°C), and imaged on a Bio-Rad MRC-600 confocal microscope. Images were obtained at least 50 μm below the slice surface and collected every 2 min as described by O'Rourke et al. (1992). Sequences were obtained from 21 slices from 21 brains. For Syto-11, cortical slices were prepared from E29, E36, and postnatal ferrets, incubated in 5 mM Syto-11 (Molecular Probes) in HBSS for 5 min on ice, rinsed in cold HBSS, and imaged by time-lapse microscopy as described above. The number of divisions imaged was 211, in 34 slices from 34 animals.

Toluidine Blue Staining of Fixed Plastic-Embedded Sections

Three E20 brains were fixed by immersion in 1% glutaraldehyde, 4% paraformaldehyde in 0.1 M Cacodylate buffer (pH 7.3) overnight and embedded in epon–araldite. Semi-thin sections (0.5 μm) were stained with toluidine blue.

Acknowledgments

Please address correspondence to S. K. M. We thank P. Zagouras and S. Artavanis-Tsakonas for Notch1 antibodies; S. Artavanis-Tsakonas, C. Blaumueller, W. Harris, and R. Dorsky for discussions about Notch; N. O'Rourke and M. Tessier-Lavigne for comments on an earlier version of the manuscript; N. O'Rourke for advice on imaging; and C. Kaznowski for assistance with histology. Supported by National Institutes of Health grant MH51864 and a National Science Foundation Presidential Faculty Fellow award to S. K. M., and by National Institute of General Medical Sciences training grant GM07365 to A. C.

Received March 6, 1995; revised June 21, 1995.

References

Artavanis-Tsakonas, S., Matsuno, K., and Fortini, M. E. (1995). Notch signalling. Science *268*, 225–232.

Berry, M., and Rogers, A. W. (1965). The migration of neuroblasts in the developing cerebral cortex. J. Anat. *99*, 691–709.

Caviness, V. S., Jr., Takahashi, T., and Nowakowski, R. S. (1995). Numbers, time, and neocortical neuronogenesis: a general developmental and evolutionary model. Trends Neurosci., in press.

Coffman, C. R., Skoglund, P., Harris, W. A., and Kintner, C. R. (1993). Expression of an extracellular deletion of *Xotch* diverts cell fate in Xenopus embryos. Cell *73*, 659–671.

Dailey, M. E., Buchanan, J., Bergles, D. E., and Smith, S. J. (1994). Mossy fiber growth and synaptogenesis in rat hippocampal slices in vitro. J. Neurosci. *14*, 1060–1078.

Doe, C. Q., and Goodman, C. S. (1985). Early events in insect neurogenesis. II. The role of cell interactions and cell lineage in the determination of neuronal precursor cells. Dev. Biol. *111*, 206–219.

Dorsky, R. I., Rapaport, D. H., and Harris, W. A. (1995). Xotch inhibits cell differentiation in the Xenopus retina. Neuron *14*, 487–496.

Fortini, M. E., Rebay, I., Caron, L. A., and Artavanis-Tsakonas, S. (1993). An activated Notch receptor blocks cell-fate commitment in the developing *Drosophila* eye. Nature *365*, 555–557.

Fujita, S. (1964). Analysis of neuron differentiation in the central nervous system by tritiated thymidine autoradiography. J. Comp. Neurol. *122*, 311–328.

Gray, G. E., and Sanes, J. R. (1992). Lineage of radial glia in the chicken optic tectum. Development *114*, 271–283.

Hicks, S. P., and D'Amato, C. J. (1968). Cell migrations to the isocortex in the rat. Anat. Rec. *160*, 619–634.

Hinds, J. W., and Ruffett, T. L. (1971). Cell proliferation in the neural tube: an electron microscopic and Golgi analysis in the mouse cerebral vesicle. Z. Zellforsch. Mikrosk. Anat. *115*, 226–264.

Langman, J., Guerrant, R. L., and Freeman, B. G. (1966). Behavior of neuro-epithelial cells during closure of the neural tube. J. Comp. Neurol. *127*, 399–411.

Levine, S. M., and Goldman, J. E. (1988). Spatial and temporal patterns of oligodendrocyte differentiation in rat cerebrum and cerebellum. J. Comp. Neurol. *277*, 441–455.

Luskin, M. B., Pearlman, A. L., and Sanes, J. R. (1988). Cell lineage in the cerebral cortex of the mouse studied in vivo and in vitro with a recombinant retrovirus. Neuron *1*, 635–647.

Martin, A. H. (1967). Significance of mitotic spindle fibre orientation in the neural tube. Nature *216*, 1133–1134.

McConnell, S. K. (1988a). Development and decision-making in the mammalian cerebral cortex. Brain Res. Rev. *13*, 1–23.

McConnell, S. K. (1988b). Fates of visual cortical neurons in the ferret after isochronic and heterochronic transplantation. J. Neurosci. *8*, 945–974.

McConnell, S. K., and Kaznowski, C. E. (1991). Cell cycle dependence of laminar determination in developing cerebral cortex. Science *254*, 282–285.

Miller, M. W. (1985). Cogeneration of retrogradely labeled corticocortical projection and GABA-immunoreactive local circuit neurons in cerebral cortex. Dev. Brain Res. *23*, 187–192.

Misson, J. P., Edwards, M. A., Yamamoto, M., and Caviness, V. J. (1988). Identification of radial glial cells within the developing murine central nervous system: studies based upon a new immunohistochemical marker. Dev. Brain Res. *44*, 95–108.

Nye, J. S., Kopan, R., and Axel, R. (1994). An activated Notch suppresses neurogenesis and myogenesis but not gliogenesis in mammalian cells. Development *120*, 2421–2430.

O'Rourke, N. A., Dailey, M. E., Smith, S. J., and McConnell, S. K. (1992). Diverse migratory pathways in the developing cerebral cortex. Science *258*, 299–302.

Price, J., and Thurlow, L. (1988). Cell lineage in the rat cerebral cortex: a study using retroviral-mediated gene transfer. Development *104*, 473–482.

Rakic, P. (1988). Specification of cerebral cortical areas. Science *241*, 170–176.

Rhyu, M. S., Jan, L. Y., and Jan, Y. N. (1994). Asymmetric distribution of numb protein during division of the sensory organ precursor cell confers distinct fates to daughter cells. Cell *76*, 477–491.

Roberts, J. S., O'Rourke, N. A., and McConnell, S. K. (1993). Cell migration in cultured cerebral cortical slices. Dev. Biol. *155*, 396–408.

Schulze, E., and Kirschner, M. (1986). Microtubule dynamics in interphase cells. J. Cell Biol. *102*, 1020–1031.

Sidman, R. L., Miale, I. L., and Feder, N. (1959). Cell proliferation and migration in the primitive ependymal zone: an autoradiographic study of histogenesis in the nervous system. Exp. Neurol. *1*, 322–333.

Smart, I. H. (1973). Proliferative characteristics of the ependymal layer during the early development of the mouse neocortex: a pilot study based on recording the number, location and plane of cleavage of mitotic figures. J. Anat. *116*, 67–91.

Spana, E. P., and Doe, C. Q. (1995). The prospero transcription factor is asymmetrically localized to the cell cortex during neuroblast mitosis in *Drosophila*. Development, in press.

Stensaas, L. J., and Stensaas, S. S. (1968). An electron microscope study of cells in the matrix and intermediate laminae of the cerebral hemisphere of the 45 mm rabbit embryo. Z. Zellforsch. *91*, 341–365.

Struhl, G., Fitzgerald, K., and Greenwald, I. (1993). Intrinsic activity of the Lin-12 and Notch intracellular domains in vivo. Cell *74*, 331–345.

Swiatek, P. J., Lindsell, C. E., Franco del Amo, F., Weinmaster, G., and Gridley, T. (1994). Notch1 is essential for postimplantation development in mice. Genes Dev. *8*, 707–719.

Takahashi, T., Nowakowski, R. S., and Caviness, V. S., Jr. (1993). Cell cycle parameters and patterns of nuclear movement in the neocortical proliferative zone of the fetal mouse. J. Neurosci. *13*, 820–833.

Voigt, T. (1989). Development of glial cells in the cerebral wall of ferrets: direct tracing of their transformation from radial glia into astrocytes. J. Comp. Neurol. *289*, 74–88.

Walsh, C., and Cepko, C. L. (1988). Clonally related cortical cells show several migration patterns. Science *241*, 1342–1345.

Weinmaster, G., Roberts, V. J., and Lemke, G. (1991). A homolog of *Drosophila Notch* expressed during mammalian development. Development *113*, 199–205.

Weinmaster, G., Roberts, V. J., and Lemke, G. (1992). *Notch2*: a second mammalian *Notch* gene. Development *116*, 931–941.

Woods, D. F., and Bryant, P. J. (1993). Apical junctions and cell signalling in epithelia. J. Cell Sci. (Suppl.) *17*, 171–181.

Zamenhof, S. (1986). Quantitative studies of mitoses in fetal rat brain: orientations of the spindles. Dev. Brain Res. *31*, 143–146.